Peridynamic modeling of concrete structures

Walter H. Gerstle & Nicolas Sau
University of New Mexico, Albuquerque, New Mexico, U.S.A.

ABSTRACT: The peridynamic model is applied to the computational analysis of plain and reinforced concrete structures. The peridynamic model is essentially a size-scaleable, continuum version of a molecular dynamics model. No assumption about the continuity of displacements is required in the model. While the continuum mechanics model requires concepts of stress and strain, the peridynamic model does not. Elasticity, cracking, and distributed damage emerge naturally from the peridynamic theory. The basic theory and several example problems are presented. The peridynamic model is promising from both conceptual and computational points of view for simulating the behavior of reinforced concrete structures.

Keywords: reinforced concrete, concrete, peridynamic, fracture, crack, nonlocal, computational mechanics, bond-slip, anchor

1 INTRODUCTION

1.1 *Why concrete is difficult to model*

Concrete is difficult to model because it is a so-called "strain-softening material". In such materials, subsequent to reaching the tensile strength, the strains localize to become what are commonly called cracks and shear bands. To prevent these cracks and shear bands from deforming excessively, reinforcing steel is usually provided in concrete structures. Due to the complexity of the interaction between the concrete and the reinforcing steel, a large number of cracks can form at significantly differing size scales. Using the finite element method (FEM), cracks can be modeled either discretely or in a smeared fashion. With the discrete crack model, the geometric continuum is altered to allow cracks to be modeled on the boundary. With the smeared crack model, on the other hand, the geometric domain of the continuum remains unchanged, but the material properties are changed to reflect the presence of damaged material regions. Neither the smeared crack nor the discrete crack approach is fully satisfactory for modeling the behavior of reinforced concrete structures at all size scales.

1.2 *FEM, continuum mechanics, and fracture mechanics*

Typically, computational continuum mechanics starts with an assumption of a spatially continuous and differentiable displacement field. Strains are obtained from spatial derivatives of the displacement field. Stresses are related to strains via Hooke's law or some nonlinear constitutive relation. Newton's second Law, F = ma, is then applied to a differential free body, resulting in the differential equations of either static or dynamic equilibrium. These differential equations are then approximately satisfied on the analysis domain, subject to specified initial and prescribed conditions.

The finite element method is similarly based upon the assumption of continuity of displacements, as well as continuity of a specified number of displacement derivatives, within the domain of the analysis.

Likewise, classical fracture mechanics is founded upon the assumption that the theory of continuum elasticity holds within the domain of analysis, and a crack is modeled as a boundary feature of the elastic domain to be simulated.

Recently, in order to regularize the finite element method when used in a smeared cracking context, nonlocal damage mechanics has been employed (Bazant & Jirasek 2002).

These fracture mechanics, damage mechanics, and nonlocal continuum mechanics approaches to compensate for the shortcomings of the assumptions of continuum mechanics theory have become complex and top-heavy, and there is a simpler approach that can be taken, called the peridynamic (near-force) method, described in the next section.

2 THE PERIDYNAMIC MODEL

2.1 *Overview of the model*

Recently, a fundamental method, called the peridynamic model (Silling 1998; 2000; 2002A; 2002B; Silling et al. 2003) for computational mechanical analysis as been introduced that makes no assumption of continuity of displacements. Thus, continuous and discontinuous (cracking and fragmentation) behavior can be handled using a single, simple paradigm. The method, which can be thought of as a size-scalable computational molecular dynamics approach, lends itself well to the modeling of reinforced concrete structures. The method is of the class of nonlocal models (Bazant and Jirasek 2002).

The peridynamic model makes no assumption of continuous or small deformation behavior. It has no requirement for the concepts of stress and strain. The peridynamic model starts with the assumption that Newton's second law holds true on every infinitesimally small freebody (or particle) within the domain of analysis. A force density function, called the pairwise force function, (with units of force per unit volume per unit volume) between each pair of infinitesimally small particles is postulated to act if the particles are closer together than some finite distance, called the material horizon. The pairwise force function may be assumed to be a function of the relative position and the relative displacement between the two particles. A spatial integration process is employed to determine the total force acting upon each particle, and a time integration process is employed to track the positions of the particles due to the applied body forces and applied displacements. One of the advantages of the peridynamic approach is that no finite element meshes are required. It is truly a meshless method.

As described by Silling (Silling 1998; Silling 2002A; Silling 2002B; Silling et al. 2003), the peridynamic model may be implemented on the computer essentially as a grid of interacting discrete particles in a 3D geometrical space.

2.2 *Basic Theory*

Refer to Figure 1 for terminology. We assume that Newton's second law holds true on an infinitesimally small particle, dV_i, of mass dm_i, undeformed position $\underline{\mathbf{x}}_i$, and displacement, $\underline{\mathbf{u}}_i$, located within domain, R:

$$\left(dm_i\right)\underline{\ddot{u}}_i = \underline{\sum\left(dF\right)}, \tag{1}$$

where $\underline{\sum\left(dF\right)}$ is the force vector acting on the free body, and $\underline{\ddot{u}}_i$ is particle i's acceleration. (The underscore signifies a vector quantity, while the over dot signifies differentiation with respect to time.)

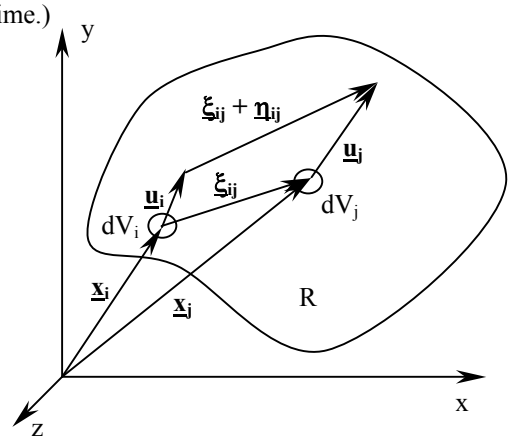

Figure 1. Terminology for peridynamic model.

Dividing both sides of Equation 1 by the differential volume of particle i, dV_i, and partitioning the force into components internal and external to the system of particles under consideration gives

$$\rho\underline{\ddot{u}} = \underline{L} + \underline{b}, \tag{2}$$

where ρ is the mass density at position $\underline{\mathbf{x}}_i$, $\underline{L}$ is the force vector per unit volume due to interaction with all other particles (for example, particle j) in domain R, and $\underline{b}$ is the externally applied body force vector per unit volume.

The internal material force density per unit volume, $\underline{L}$, acting upon particle i, is an integral over all other particles, j, within the domain, R:

$$\underline{L} = \int_R \left(\underline{f_{ij}}\right) dV_j \,, \tag{3}$$

where $\underline{f_{ij}}$ is the density of force densities between dV_i and the surrounding particles, dV_j. The pairwise force function, $\underline{f_{ij}}$, which has units of force per unit volume squared, can be viewed as a material constitutive property. In the simplest case, let us assume elastic behavior. In this case

$$\underline{f_{ij}} = \underline{f_{ij}}\left(\underline{u_j} - \underline{u_i}, \underline{x_j} - \underline{x_i}\right) = \underline{f_{ij}}\left(\underline{\eta_{ij}}, \underline{\xi_{ij}}\right), \tag{4}$$

so the pairwise force function is a function of relative displacement and relative position between particles i and j. More complex constitutive relations, incorporating internal material state variables, could also be contemplated.

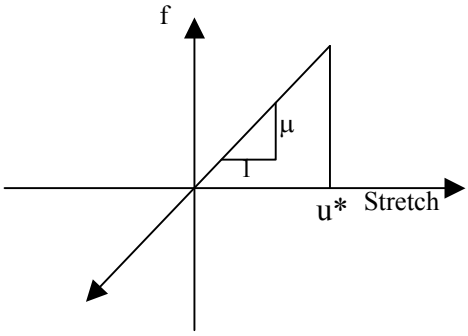

Figure 2. Micro elastic peridynamic model for plain concrete. This model governs the forces between two particles situated within the material horizon, δ, of each other.

Silling (Silling 1998) has proposed a simple nonlocal peridynamic constitutive model

$$\underline{f_{ij}}\left(\underline{\eta_{ij}}, \underline{\xi_{ij}}\right) = \frac{\mu\left(\left|\underline{\xi_{ij}} + \underline{\eta_{ij}}\right| - \left|\underline{\xi_{ij}}\right|\right)\left(\underline{\xi_{ij}} + \underline{\eta_{ij}}\right)}{\left|\underline{\xi_{ij}} + \underline{\eta_{ij}}\right|} \tag{5}$$

if $\left|\underline{\xi_{ij}} + \underline{\eta_{ij}}\right| - \left|\underline{\xi_{ij}}\right| < u^*$ and $\left|\underline{\xi_{ij}} + \underline{\eta_{ij}}\right| < \delta$. $\underline{f_{ij}}\left(\underline{\eta_{ij}}, \underline{\xi_{ij}}\right) = 0$ otherwise. Here μ, δ, and u^* are positive "microelastic" constants. Thus, the "spring" connecting any two particles is linear for small relative displacements, but it breaks when the relative displacement between the two particles exceeds u^*. Only particles within a distance from each other, δ (the material horizon), in the deformed configuration interact.

A simple micro elastic peridynamic model (with tensile limit) for concrete is shown in Figure 2. As will be demonstrated with the subsequent examples, this model appears to be sufficiently comprehensive to model concrete elasticity, tensile fracture, shear bands, and crushing.

3 NUMERICAL IMPLEMENTATION

3.1 *Approach used in Emu*

Emu is the name of the software program created by Silling [Silling 1998], and used to model the examples shown in this paper. In Emu, a cubical grid of nodes spaced equally in all dimensions serves as the base space for describing particle motion. Material properties and applied displacement and velocity initial and prescribed conditions and applied body loadings are defined using sequentially numbered primitive regions, as shown in Figure 3. A node inherits material properties and prescribed conditions from the first region within which the node appears. Nodes not contained within regions are ignored in the computations.

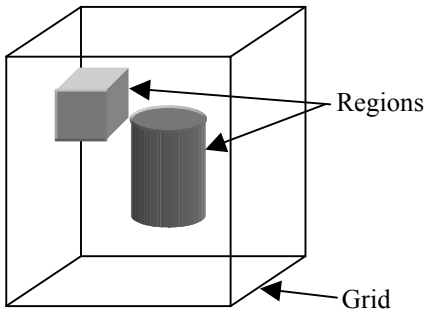

Figure 3. Approach to structural modeling used by Emu.

Time steps are automatically computed based upon time integration stability requirements. The material horizon, δ, is automatically chosen to be approximately three times the node grid spacing, to ensure that a sufficient number of nodes are included to provide a reasonable approximation to the integrated force acting on each particle, based upon Equation 3. The microelastic stiffness, μ, the microelastic bond-breaking distance, u*, and the material horizon, δ, are automatically be altered to account for differing grid spacings.

Emu can be run on a multiple processor high-performance parallel computer; however each of the examples shown in this paper was run on a single processor computer in less than four hours.

3.2 *Possible peridynamic modeling strategies*

Emu currently makes use of a structured cubical background grid, using an explicit time integration approach. This is a highly robust modeling approach, but rather inefficient for solution of static problems. To improve computational efficiency, it is possible to employ mapped material regions of varying dimensionality and shape. Each material region shown in Figure 3 could also be individually discretized with mapped nodes, as described in [Gerstle 2002]. For material regions modeled with dimensionality less than three, it will be necessary to add rotational degrees of freedom to the nodes, to allow moments to be sustained by the material. For example, to model reinforced concrete structures, it will be efficacious to model reinforcement as a one-dimensional domain, while the concrete would be modeled as either a two-dimensional (membrane, plate or shell) or a three-dimensional (solid) domain.

The resulting equations are highly nonlinear due to the micro elastic model depicted in Figure 2. While an explicit time integration approach is the most stable and accurate approach, it will be useful to develop efficient quasistatic solution techniques. In such a technique, the solution would proceed as stepwise linear increments, as bonds are broken one at a time. Thus, computational time would not be wasted during time domains (or pseudo-time domains) where no bonds are being broken. Efficient methods for altering the stiffness matrix due to local bond nonlinearities can be developed.

4 EXAMPLE PROBLEMS

For simplicity in graphical depiction of the results, and to limit computer simulation times to a five-hour limit per example using a single-processor computer, all of the problems shown in this paper are two-dimensional. Only one layer of nodes in the out-of-page direction is included in each computation, to reduce computational effort required to solve the problem. Hence, the following examples are merely illustrative of the possibilities of the peridynamic model, rather than simulations of actual laboratory tests. However, with more powerful parallel-processor computers and better graphical display methods, all of these problems could have been modeled as fully three-dimensional problems.

We next simulate a uniaxial tension specimen, a uniaxial compression specimen, tensile and shear pullout of an anchor bolt, tensile pull-out of two anchor bolts, and the splice of two embedded ribbed reinforcing bars in tension.

4.1 *Uniaxial tension specimen*

This problem is a cube of concrete 2m wide by 1.2m high, in what amounts essentially to plane-strain conditions. The microelastic concrete model is shown in Figure 2, with parameters μ, u^*, and δ chosen to simulate the properties of a concrete with sound speed of 5000 m/s, and tensile strain limit of 0.000166. The bottom 0.2m of the specimen is constrained to have zero prescribed vertical velocity component, and the top 0.2m of the specimen has a prescribed downward velocity of 0.3 m/s. Figure 4 shows the Emu input file.

```
Uniaxial Tension  Specimen
processors 1 1 1
grid_dimensions 21  3 21
max_time  0.1
max_time_steps  10000
plot_dump_frequency 1000
grid_spacing  0.06
number_of_material_regions  1
material_region_geometry_1
  1  -.6  .6 -.01 .01  -1.2  0.
density_1 2400
microelastic_1  1 5000 4.14e6 0.000166
material_region_ic_1  0 0 0    0 0 0
number_of_boundary_regions  2
boundary_region_geometry_1
  1 -1. 1. -.1 .1 -1.2 -1.0
boundary_region_geometry_2
  1 -1. 1. -.1 .1 -.2   0.
boundary_condition_1  3 0 1 1 0 0 0   1.
boundary_condition_2  3 0 1 1 0 0 .3  1.
plot_all
viscous_damping_coefficient  .9
```

Figure 4. Emu input file, used to model the uniaxial tension specimen described in Section 4.1.

Figure 5 shows a plot of the bond damage plotted on the deformed shape after the top of the specimen had moved up 1.1 cm. As expected, a

horizontal tensile fracture develops (near the top of the specimen). The computed behavior appears to be entirely plausible.

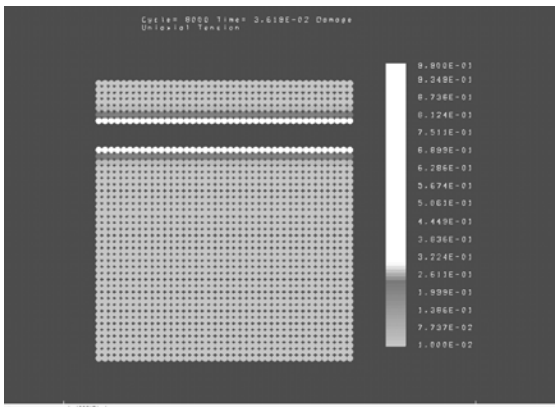

Figure 5. Uniaxial tension specimen; damage shown (as color bands) on magnified deformed shape.

4.2*Uniaxial compression specimen*

This problem is identical to the uniaxial tension problem described in the previous section, with the exception that the prescribed velocity at the top of the specimen is now down, rather than up, and also a small material region of reduced stiffness was introduced near the top left-hand side of the specimen to induce a small initial asymmetry.

Figure 6 shows a picture of the damage plotted as color bands on the (magnified) deformed shape after the top of the specimen had moved down 1.2 cm. Notice the diagonal shear bands that form, as well as the dynamic ejection of crushed material from the top sides of the specimen. The computed behavior appears to be entirely plausible.

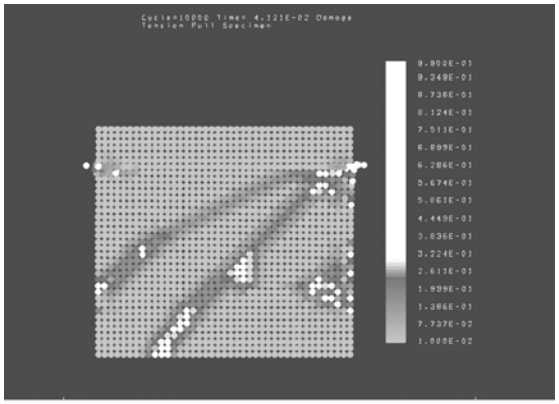

Figure 6. Uniaxial compression specimen; damage shown (as color bands) on magnified deformed shape.

The width of the shear band is essentially governed by the value of the material horizon, δ. However, as mentioned earlier, the material horizon δ is chosen to be three times the nodal spacing. In concrete, there is an actual physical material horizon that is approximately governed by the aggregate size. Therefore, the width of the shear bands indicated in Figure 6 is perhaps larger than would be predicted if a finer mesh were employed. Further research should clarify convergence characteristics of the peridynamic approach.

4.3 *Anchor bolt pullout in tension and shear*

A more complex situation is involved in the pullout of a steel anchor bolt, shown in Figure 7(a). The pullout rate is 0.3 m/s. Again using a two-dimensional plane strain simulation of what is an essentially three-dimensional problem, the damage and deformed shape of the pullout of a steel bolt is shown in Figure 7(b).

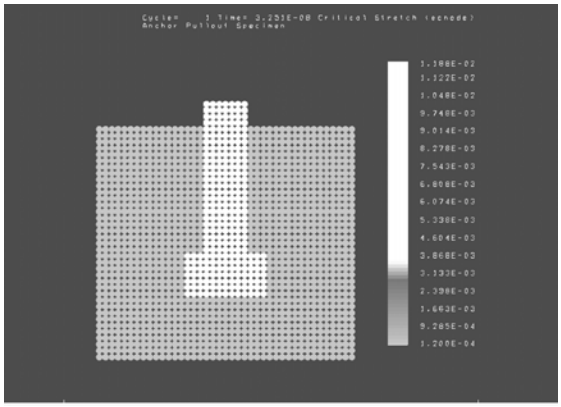

Figure 7(a). Anchor pullout problem: undeformed shape.

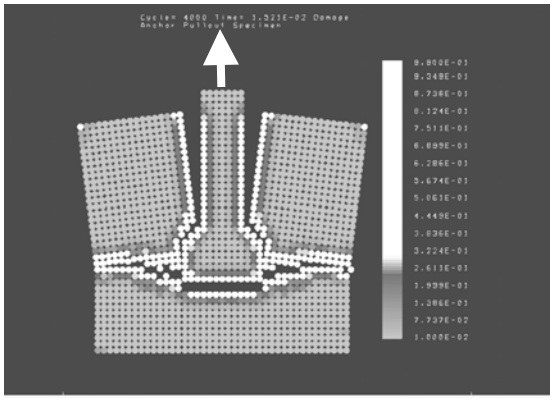

Figure 7(b). Anchor pullout problem: color plot of damage on magnified deformed shape.

The concrete properties are the same as those in the previous examples, and the steel bolt is given a sufficiently high yield strength that it does not yield. The geometric dimensions of the concrete are essentially that same as in the previous examples. As is evident from Figure 7(b), there is damage adjacent to the steel anchor bolt, as well as horizontal and vertical planes of damage adjacent to the anchor bolt.

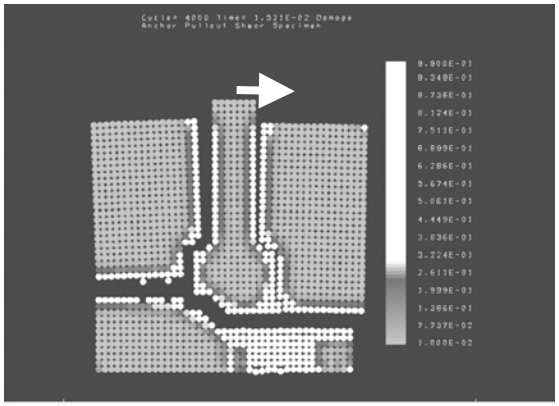

Figure 8. Anchor shear problem: plot of damage on magnified deformed shape.

In Fig. 8, the anchor bolt simulation is repeated, with the difference that the applied velocity at the top of the bolt is now to the right. Zones of damage appear as lighter and darker zones in the figure.

4.4 *Pullout of two anchor bolts*

Figures 9(a) and 9(b) show successive deformed shapes of a 1.2m wide by 1m high concrete specimen with two embedded anchor bolts pulled at 0.3 m/s in opposing vertical directions. Tensile cracks, shear cracks, and shear bands are evident.

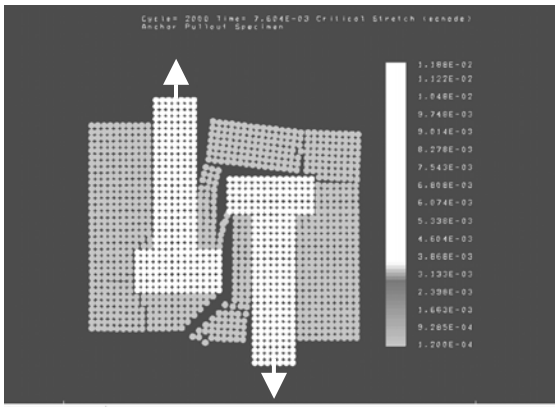

Figure 9(a). Bond-slip: magnified deformed shape, at early stage of damage.

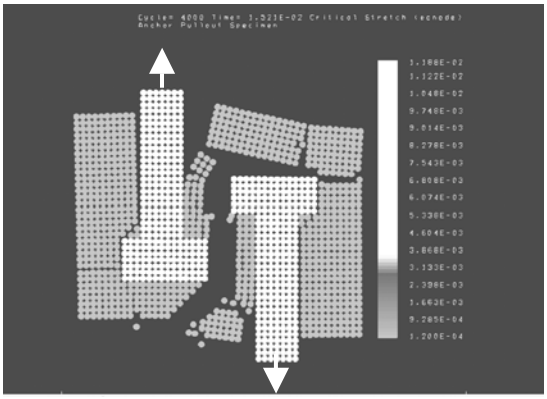

Figure 9(b). Bond-slip: magnified deformed shape, at later stage of damage.

4.5 *Splice of ribbed reinforcing bars*

Figures 10 and 11 each show three successive deformed shapes of a two-dimensional representation of a splice between two ribbed reinforcing bars embedded in concrete and pulled in opposing directions. The only difference between the simulation depicted in Figure 10 and that depicted in Figure 11 is that the grid spacing is refined by a factor of two in the latter figure.

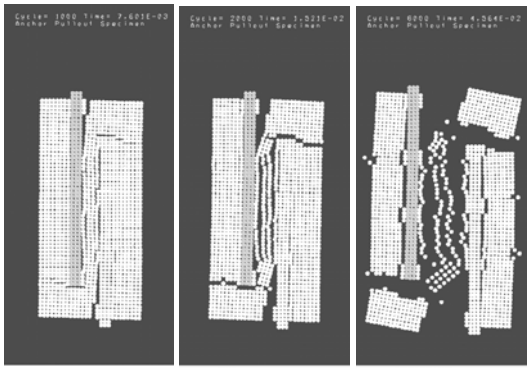

(a) (b) (c)

Figure 10. Magnified deformed shapes of splice of reinforcing bars in concrete at three stages (coarse discretization – grid spacing is 0.06 m).

These figures show essentially the same deformation mechanisms despite the differing discretization scales, giving some evidence that the deformation mechanisms are in fact objective, and independent of the discretization. Furthermore, the results seem to be reasonable in light of the authors' observations of laboratory experiments.

Further development is necessary to determine if in fact the implementation of the peridynamic model developed in Emu can yield truly objective results, with detailed predictive capability.

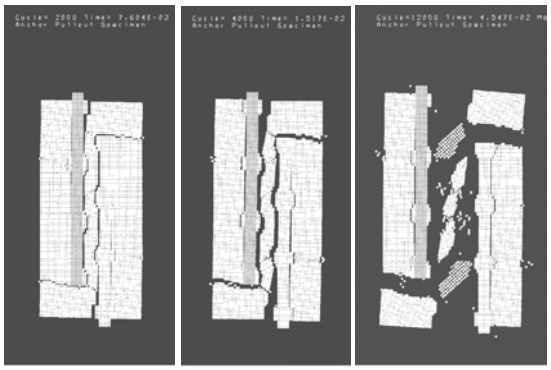

(a) (b) (c)

Figure 11. Magnified deformed shapes of splice of reinforcing bars in concrete at three stages (fine discretization – grid spacing is 0.03 m).

5 CONCLUSIONS

The peridynamic model provides an alternative approach to the modeling of reinforced concrete that avoids any presumption of a continuous displacement field. Neither the concept of strain nor the concept of stress is required by this model.

Promising features of the peridynamic model include:

- A simple conceptual model.
- A relatively simple constitutive microelastic model has the potential to represent cracking, and damage at the macro scale.
- Bond-slip behavior between the concrete and the steel reinforcement emerges naturally, without resorting to any special models.
- Size scaling appears to be uncomplicated. However, further research is required.
- Very fine grids are unnecessary, unless, of course, high spatial resolution of the damage is required. Again, further research is in order.
- Large deformations are naturally modeled; no assumption of small deformations is required.

There are some disadvantages of the peridynamic model as well:

- The model does not yield analytical solutions. Therefore, it is essentially a *computational* model.
- For elastic cases in which no damage is present, it is probably not as efficient as the conventional finite element approach
- As the grid is refined spatially, the stable time step size is also decreased. Thus, the number of computations required increases dramatically with grid refinement. (Of course, this is also true with any other method of computational modeling.)

Some research issues to be resolved include:

- Development of microelastic, microplastic, and rate-sensitive peridynamic models.
- Development of models including dimension simplification: bars, beams, plates, and shells.
- Development of rigorous convergence estimates. Can any convergence guarantees be developed?
- Development of efficient solution algorithms.

ACKNOWLEDGMENTS

The generosity of Stewart Silling in the form of several helpful discussions and in sharing the software Emu is appreciated. The author became aware of the peridynamic model while employed during the summer of 2003 at Sandia National Laboratories.

REFERENCES

Bazant, Z. P., and Jirasek, M., "Nonlocal Integral Formulations of Plasticity and Damage: Survey of Progress", Journal of Engineering Mechanics, Vol. 128, No. 11, pp. 119-1149, Nov. 2002.

Gerstle, W., "Toward a Meta-Model for Computational Engineering", Engineering with Computers, Vol. 18, Issue 4, pp 328-338, Springer-Verlag, London, 2002.

Silling, S. A. "Reformation of Elasticity Theory for Discontinuous and Long-Range Forces", SAND98-2176, Sandia National Laboratories, Albuquerque, NM., 1998.

Silling, S. A. "Reformulation of Elasticity Theory for Discontinuities and Long-Range Forces", Journal of the Mechanics and Physics of Solids, Vol. 48: pp. 175-209, 2000.

Silling, S. A., "Dynamic Fracture Modeling With a Meshfree Peridynamic Code", SAND2002-2959C, Sandia National Laboratories, Albuquerque, NM, 2002.

Silling, S. A., "EMU Website", SAND2002-2103P, Sandia National Laboratories, Albuquerque, NM, 2002.

Silling, S. A., Zimmermann, M., and Abeyaratne, R., "Deformation of a Peridynamic Bar", SAND2003-0757, Sandia National Laboratories, Albuquerque, NM, 2003.